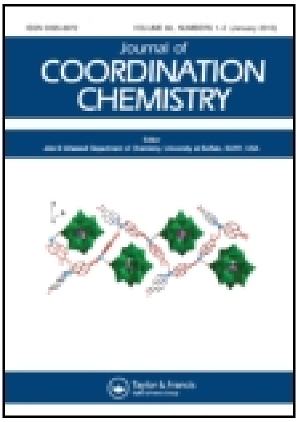

Journal of Coordination Chemistry
Publication details, including instructions for authors and subscription information:
http://www.tandfonline.com/loi/gcoo20

Pb(II) and Bi(III) complexes involving a Schiff base ligand: syntheses, structures, physical, and antioxidant properties

Wen-Ting Deng[a], Jia-Cheng Liu[abc] & Jing Cao[c]

[a] Key Laboratory of Eco-Environment-Related Polymer Materials of Ministry of Education, College of Chemistry and Chemical Engineering, Northwest Normal University, Lanzhou, P.R. China

[b] Key Laboratory of Polymer Materials of Gansu Province, College of Chemistry and Chemical Engineering, Northwest Normal University, Lanzhou, P.R. China

[c] Key Laboratory of Bio electrochemistry & Environmental Analysis of Gansu Province, College of Chemistry and Chemical Engineering, Northwest Normal University, Lanzhou, P.R. China

Accepted author version posted online: 08 Oct 2013.Published online: 15 Nov 2013.

To cite this article: Wen-Ting Deng, Jia-Cheng Liu & Jing Cao (2013) Pb(II) and Bi(III) complexes involving a Schiff base ligand: syntheses, structures, physical, and antioxidant properties, Journal of Coordination Chemistry, 66:21, 3782-3790, DOI: 10.1080/00958972.2013.852664

To link to this article: http://dx.doi.org/10.1080/00958972.2013.852664

Journal of Coordination Chemistry, 2013
Vol. 66, No. 21, 3782–3790, http://dx.doi.org/10.1080/00958972.2013.852664

Pb(II) and Bi(III) complexes involving a Schiff base ligand: syntheses, structures, physical, and antioxidant properties

WEN-TING DENG†, JIA-CHENG LIU*†‡§ and JING CAO§

†Key Laboratory of Eco-Environment-Related Polymer Materials of Ministry of Education, College of Chemistry and Chemical Engineering, Northwest Normal University, Lanzhou, P.R. China
‡Key Laboratory of Polymer Materials of Gansu Province, College of Chemistry and Chemical Engineering, Northwest Normal University, Lanzhou, P.R. China
§Key Laboratory of Bio electrochemistry & Environmental Analysis of Gansu Province, College of Chemistry and Chemical Engineering, Northwest Normal University, Lanzhou, P.R. China

(*Received 30 July 2013; accepted 18 September 2013*)

Two new complexes, $\{[Pb\mathbf{L}(NO_3)_2H_2O]H_2O\}_n$ (**1**) and $[Bi\mathbf{L}_2(NO_3)_2]NO_3$ (**2**), based on (E)-3-chloro-6-[2-(pyrazin-2-ylmethylene)hydrazinyl]pyridazine (**L**) were synthesized and characterized by IR spectra, single-crystal X-ray diffraction, and elemental analyzes. X-ray single crystal diffraction experiments of **1** and **2** display that extensive hydrogen bonds and $\pi \ldots \pi$ stacking interactions construct the 1-D infinite chain $\{[Pb\mathbf{L}(NO_3)_2H_2O]H_2O\}_n$ and $[Bi\mathbf{L}_2(NO_3)_2]NO_3$ into two 3-D supramolecular frameworks. Interestingly, pure phase PbO nano-particles were synthesized by thermolysis of **1** and characterized by scanning electron microscopy and X-ray powder diffraction analyzes. Furthermore, antioxidant activities of **L**, **1,** and **2** were also studied.

Keywords: Schiff base; Pb(II) and Bi(III) Complexes; Physical and antioxidant properties

1. Introduction

Constructing new coordination polymers and modifying their architectures to understand how molecules can be assembled and how functions can be achieved have attracted attention [1–9]. It is well accepted that the coordination spheres of lead(II) and bismuth(III) are generally determined by the stereo-activity of the valence shell lone electron pairs, although it is somewhat difficult to prove. Many attempts have been made to exhibit variable coordination geometries of lead(II) and bismuth(III) complexes and probe their properties using physical and/or chemical methods. For example, employing a series of new lead(II) coordination polymers as precursors for the preparation of nano-structured PbO particles by thermolyses in oleic acid at 180 and 200 °C, has been reported [10, 11]. In addition, bismuth-containing compounds applied in medicine have a long history and remain scantily explored, although the use of heavy metals was reduced in the last two decades [12, 13].

We recently described five new copper(II) complexes based on a Schiff base (E)-3-chloro-6-[2-(pyrazin-2-ylmethylene)hydrazinyl]pyridazine (**L**, shown in scheme 1), with

---

*Corresponding author. Email: jcliu8@nwnu.edu.cn

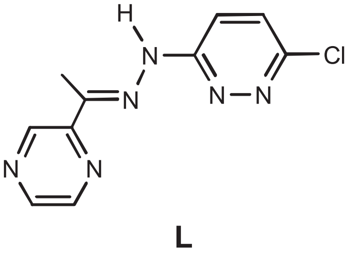

Scheme 1. The structure of **L**.

which coordination modes of different copper(II) salts were explored [14]. To further probe and understand the fascinating structures and properties of Pb(II) and Bi(III) complexes, we herein report extension of our investigations on the coordination chemistry of **L** with Pb $(NO_3)_2$ and $Bi(NO_3)_2$, and discuss the structures of the obtained two new complexes, $\{[Pb\mathbf{L}(NO_3)_2H_2O]H_2O\}_n$ (**1**) and $[Bi\mathbf{L}_2(NO_3)_2]NO_3$ (**2**). Thermolysis of **1** and antioxidant activities of **L**, **1** and **2** were also carried out.

2. Experimental

2.1. *Materials and physical measurements*

All solvents and reagents were used directly without purification as commercial analytical grade. IR spectra were measured by a FTS 3000 (the USA DIGILAB) spectrometer as KBr pellets from 4000 to 400 cm^{-1}. Elemental analyzes of C, H, and N were recorded on a VxRio EL Instrument. X-ray powder diffraction (XRPD) measurements were performed using an X-ray diffractometer (D/Max-2400) of Rigaku.

2.2. *Synthesis of $\{[PbL(NO_3)_2H_2O]H_2O\}_n$ (1)*

L was synthesized by refluxing 1-(pyrazin-2-yl)ethanone, 3-chloro-6-hydrazinylpyridazine, and three drops of glacial acetic acid in methanol for 8 h. Yield: 85.6% [14]. A mixture of **L** (0.1 mM, 24.8 mg) and $Pb(NO_3)_2$ (0.1 mM, 33.3 mg) was placed in 20 mL methanol and mixed. Dark yellow block crystals suitable for X-ray single crystal diffraction were obtained by slow evaporation of the solution for two weeks. Yield: 54.5%. Elemental Calcd for $C_{10}H_{13}ClN_8O_8Pb$: C, 19.50; H, 2.13; N, 18.19%. Found: C, 19.32; H, 2.01; N, 18.32%. IR data (cm^{-1}): 3444 s, 1594 m, 1441 m, 1385 *versus* 13,282 m, 1143 m, 844 w.

2.3. *Synthesis of $[BiL_2(NO_3)_2]NO_3$ (2)*

The synthesis of **2** was similar to that of **1**, except that $Bi(NO_3)_3{\cdot}5H_2O$ (0.05 mM, 24.2 mg) was added instead of $Pb(NO_3)_2$. Red block crystals were obtained by slow evaporation of the solution for three weeks in 48.4% yield. Elemental Calcd for $C_{20}H_{18}BiCl_2N_{15}O_9$: C, 26.92; H, 2.03; N, 23.54%. Found: C, 27.02; H, 1.91; N, 23.62%. IR data (cm^{-1}): 3440 s *versus* 3604 m, 1450 m, 1385 *versus* 1285 m, 1148 m, 842 w.

2.4. *Synthesis of PbO nano-particles*

The precursor of **1** (0.1 mM) was dissolved in 2 mL oleic acid and degassed for 20 min. Then the solution was heated to 180 °C for 2 h. Obtained black precipitate was added to a small amount of toluene and a large excess of EtOH. PbO nano-particles were separated by centrifugation, washed by EtOH, and dried under air.

2.5. *X-ray data collection and structure refinement*

X-ray diffraction analysis data of **1** and **2** were collected with a Bruker SMART APEX II diffractometer with graphite-monochromated Mo Kα radiation (λ = 0.71073 Å) by θ scan mode. The structures were solved by direct methods with *SHELXS-97* and refined with full-matrix least-squares using *SHELXL-97* [15]. All non-hydrogen atoms were refined anisotropically; all hydrogens were fixed geometrically at calculated distances and refined isotropically. The detailed crystallographic data and structure refinements for **1** and **2** are given in table S1, while selected bond lengths and angles are presented in tables S2 and S3.

2.6. *Scavenger measurements of superoxide radical and hydroxyl radical*

The superoxide radicals were measured in the test system using nitroblue tetrazolium, Vitamin B_2, and methionine (NBT/VitB2/MET) [16]. **L**, **1**, and **2** dissolved in DMF ($C_{i(i\,=\,1\text{–}5)}$ = 0.2, 1.0, 2.0, 3.0, and 4.0 μM), respectively, were added to solution containing MET (0.01 M L^{-1}), NBT (4.6 × 10^{-5} M L^{-1}), VitB_2 (3.3 × 10^{-6} M L^{-1}), and phosphate buffer (0.067 M L^{-1}). After incubating the mixture solution at 30 °C for 10 min and illuminating with a fluorescent lamp for 3 min, the absorbance (A_i) of the samples was measured at 560 nm. The suppression ratio was calculated by using the following equation:

$$\text{Suppression ratio}(\%) = [(A_0 - A_i)/(A_0)] \times 100\%$$

where A_i is the absorbance in the presence of **L**, **1**, and **2**, and A_0 is the absorbance in the absence of **L**, **1**, and **2**.

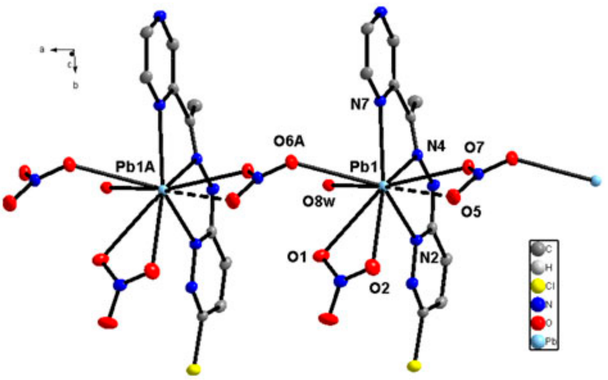

Figure 1. Crystal structure of **1** with 10% thermal ellipsoids (symmetry code: A 1 + x, y, z). All hydrogens and one free water are neglected for clarity.

The hydroxyl radical scavenging study was prepared through the Fenton reaction [17]. **L**, **1,** and **2** were dissolved in DMF ($C_{i(i=1-5)} = 2.0$, 4.0, 6.0, 8.0, and 10.0 µM), respectively. Safranine (0.5 mL, 114 µM), 1 mL 945 µM EDTA-Fe(II), 1 mL 3% H_2O_2, and 2.5 mL 0.15 M phosphate buffer (pH 7.4) were added to the 30 µL test solution. The sample without the tested compounds was used as the control. The resulting mixture was incubated for 1 h at 37 °C. Then a UV spectrophotometer was used to measure the absorbance at 520 nm (A_i, A_0, A_c). The suppression ratio was calculated by using the following equation:

$$\text{Suppression ratio}(\%) = [(A_i - A_0)/(A_c - A_0)] \times 100\%$$

where A_i is the absorbance in the presence of **L**, **1,** and **2;** A_0 is the absorbance in the absence of **L**, **1,** and **2**; and A_c is the absorbance in the absence of **L**, **1,** and **2**, EDTA-Fe (II) and H_2O_2.

The antioxidant activity was described as the 50% inhibitory concentration (IC_{50}). IC_{50} values were calculated from regression lines where x was the concentration of **L**, **1,** and **2** in µM and y was the percent inhibition of **L**, **1,** and **2**.

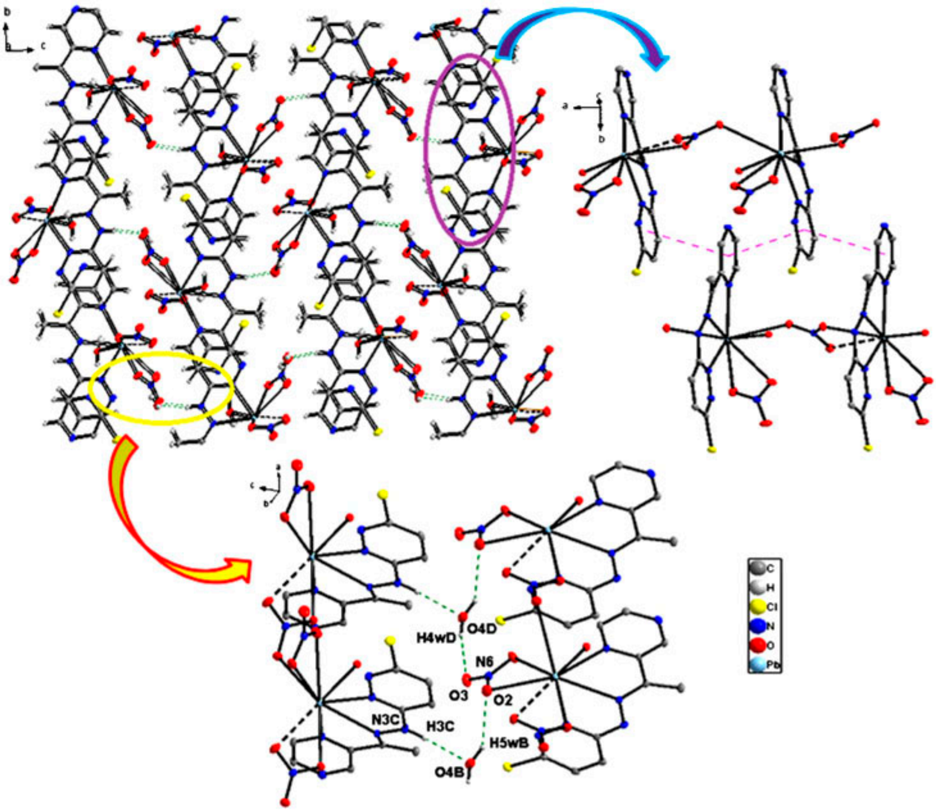

Figure 2. The 3-D supramolecular structure of **1** obtained by hydrogen bonds and offset $\pi \ldots \pi$ stacking interactions.

3. Results and discussion

3.1. *Structure of {[PbL(NO_3)$_2$$H_2O$]$H_2O$}$_n$ (1)*

As shown in figure 1, the crystal structure of **1** reveals that each Pb(II) is bonded to three nitrogens of **L** and five oxygens from three nitrates and one coordinated water. In one asymmetric unit, the nitrates exhibit two different coordination modes; one nitrate is bidentate to Pb(II) and the other as bidentate chelating and bridging links two neighboring **L** to form a 1-D infinite chain. The intramolecular Pb1…Pb1A separation is 6.8340(7) Å. Coordination number of Pb(II) of 2–5 shows hemidirected stereochemistry, high coordination number (9,10), holodirected geometry, and coordination number (6–8) either hemidirected or holodirected geometry [18]. In this structure, the lone pair of electrons on Pb1 can

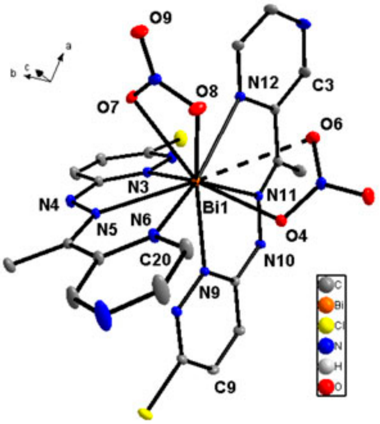

Figure 3. Crystal structure of **2** with 10% thermal ellipsoids. All hydrogens and one free nitrate are neglected for clarity.

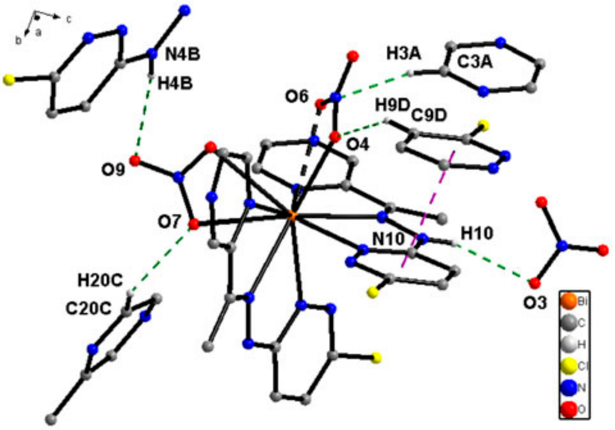

Figure 4. The 3-D supramolecular structure of **2** obtained by hydrogen bonds and offset $\pi \ldots \pi$ stacking interactions.

be considered to locate opposite of Pb1–N4 and close to the weak bond of Pb1–O5 with longer distance of 3.167(5) Å. The bond angles around Pb(II) are 43.27(14)–159.25(14)°. The coordination sphere of each Pb(II) is hemidirected. Hydrogen bond interactions (O–H…O and N–H…O, figure 2 and table S4) and offset $\pi \ldots \pi$ stacking of neighboring pyridazinyl and pyrazinyl rings with a sandwich conformation (figure 2 and table S5) stabilize the crystal lattice in a 3-D supramolecular framework in the solid state.

3.2. *Structure of [BiL$_2$(NO$_3$)$_2$]NO$_3$ (2)*

The X-ray single-crystal structure of **2** is shown in figure 3. Selected bond lengths and angles are given in table S3. The asymmetric unit consists of two **L**, one Bi(III), two coordinated nitrates, and one free nitrate. Each Bi(III) is chelated by six nitrogens of two **L** with Bi–N distances 2.396(7)–2.698(8) Å, and bonded to three oxygens from two bidentate

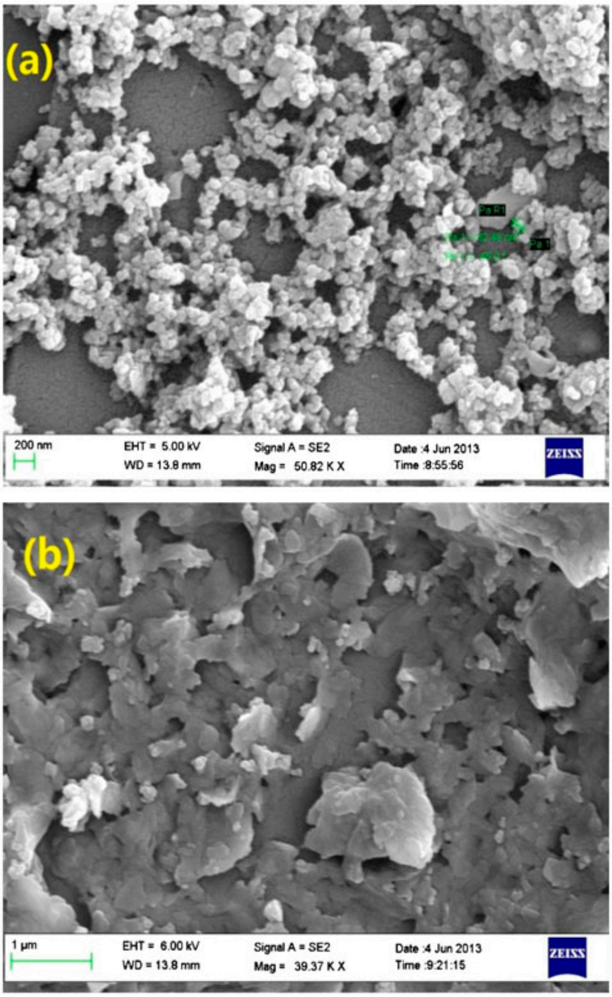

Figure 5. SEM images of PbO nano-particles obtained by thermolysis of **1** at 180 °C (a) and 200 °C (b).

nitrates with Bi–O distances from 2.482(7) to 2.684(8) Å. The weak bond of Bi1–O6 at 3.042(5) Å can be attributed to the effects of a lone pair of electrons on Bi(III). The coordination sphere of Bi1 can be considered as hemidirected, and the lone pair of electrons should mainly locate close to the weak bond of Bi1–O6 [19, 20]. In one asymmetric unit, the dihedral angle of the neighboring **L** is about 88.2°. The $[Bi\mathbf{L}_2(NO_3)_2]NO_3$ units are further joined together by the hydrogen bonds of C–H…N, C–H…O, and N–H…O (figure 4 and table S4) and offset $\pi \ldots \pi$ stacking of neighboring pyridazinyl rings (figure 4 and table S5) to organize a 3-D supramolecular framework in the solid state.

3.3. *PXRD patterns*

The phase purifies of **1** and **2** were confirmed by X-ray powder diffraction (XRPD) analyzes at room temperature. As shown in figure S1, the results show that the synthesized materials exhibit good agreement with the simulated values of respective single crystal structures, indicating that **1** and **2** are single crystalline phases.

3.4. *Description of PbO nano-particles*

As shown in figure S2, figures 5 and 6, pure phase PbO nano-particles were synthesized by decomposition of **1** as precursor in oleic acid. The temperature of thermolysis experiment was from 160 to 200 °C. At 180 °C, PbO nano-particles about 65 nm diameter (figure S2 and figure 5(a)) with good separation were produced and characterized by scanning electron microscopy (SEM) and XRPD analyzes [10, 11] [shown in figure 6]. An increasing agglomeration and large particles of PbO were also obtained at 200 °C (shown in figure 5(b)). When the temperature was under 180 °C, the decomposition of **1** did not take place. The thermolysis experiment of **2** was also carried out, but we did not obtain any similar nano-particles.

3.5. *Antioxidant activities*

Figure 7 compares the inhibitory effects of **L**, **1,** and **2** based on $O_2^{\bullet -}$ [figure 7(a)] and $^{\bullet}OH$ [figure 7(b)]. Increasing inhibitory effects against $O_2^{\bullet -}$ and $^{\bullet}OH$ are observed with

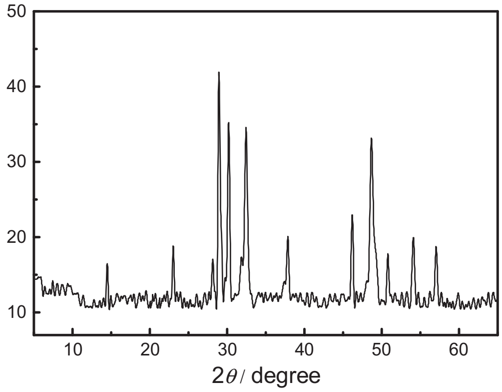

Figure 6. XRPD pattern of PbO nano-particles obtained by thermolysis of **1** at 180 °C.

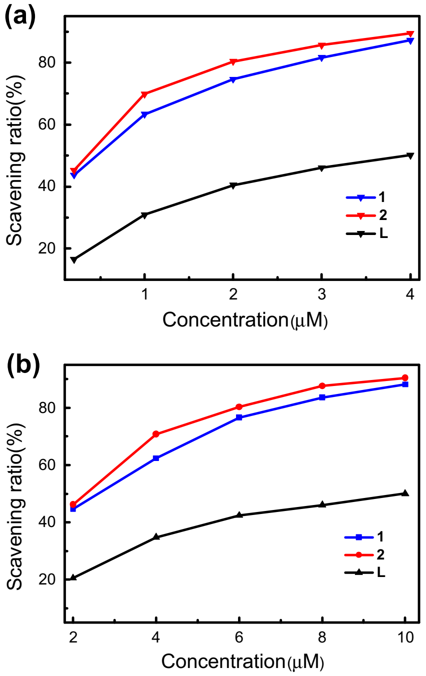

Figure 7. Scavenging effects of **L**, **1,** and **2** on $O_2^{\bullet-}$ (a) and $^{\bullet}OH$ (b).

increasing concentration of the compounds, and the suppression ratio increases when the sample concentration increases in the region of tested concentration. As shown in figure 7(a), IC_{50} value of the inhibitory effects of **L**, **1**, and **2** on $O_2^{\bullet-}$ are 4.00, 0.33, and 0.25 μM, respectively, higher superoxide dismutase activity than standard antioxidants like vitamin C (IC_{50}: 852 mM) [21]. As illustrated in figure 7(b), IC_{50} value of the inhibitory effects of **L**, **1,** and **2** against $^{\bullet}OH$ are 10.00, 2.54, 2.22 and 3.47 μM, respectively. The complexes are better antioxidants than ligand, attributed to the chelating function of organic molecules and the metal ions to achieve significantly selective effect of radical scavenging activity in biological systems [22].

4. Conclusions

We have synthesized two new complexes, $\{[Pb\mathbf{L}(NO_3)_2H_2O]H_2O\}_n$ (**1**) and $[Bi\mathbf{L}_2(NO_3)_2]NO_3$ (**2**), derived from (E)-3-chloro-6-[2-(pyrazin-2-ylmethylene)hydrazinyl]pyridazine (**L**). Due to the presence of the lone pair of electrons of metals, the hemidirected coordination spheres and lengthening bonds around metals are observed in **1** and **2**. Pure phase PbO nano-particles were obtained by thermolysis of **1**. Compared to the scavenging effects against $O_2^{\bullet-}$ and $^{\bullet}OH$ of a series of copper(II) complexes [14], **1** and **2** exhibit better activities. Moreover, **1** and **2** disclose more active scavenging effects against $O_2^{\bullet-}$ and $^{\bullet}OH$ than standard antioxidants, such as vitamin C. This feature might reflect that Pb(II) and Bi (III) complexes can be used as potential antioxidants. This work affords a basis for the preparation of new nanoscale materials and the design of potential antioxidants and therapeutic agents for some diseases.

Supplementary material

Powder X-ray diffraction patterns, and bond lengths and angles of **1** and **2**. Crystallographic data (excluding structure factors) for the structures in this article have been deposited with the Cambridge Crystallographic Data Center, CCDC, 12 Union Road, Cambridge, CB2 1EZ, UK. Copies of the data can be obtained free of charge on quoting the depository numbers CCDC-938843 (**1**) and CCDC-938844 (**2**) (Fax: +44–1223-336033; Email: deposit@ccdc.cam.ac.uk; or http://www.ccdc.cam.ac.uk). Supplemental data for this article can be accessed http://dx.doi.org/10.1080/00958972.2013.852664.

Funding

We are thankful for support of this study by the National Natural Science Foundation of China [grant number 20871099] and Gansu Provincial Natural Science Foundation of China [grant number 0710RJZA113].

References

[1] D.K. Unruh, K. Gojdas, A. Libo, T.Z. Forbes. *J. Am. Chem. Soc.*, **135**, 7398 (2013).
[2] E. Coronado, G.M. Espallargas. *Chem. Soc. Rev.*, **42**, 1525 (2013).
[3] S.J. Wang, S.S. Xiong, Z.Y. Wang, J.F. Du. *Chem. Eur. J.*, **17**, 8630 (2011).
[4] R. Patra, H.M. Titi, I. Goldberg. *Cryst. Growth Des.*, **13**, 1342 (2013).
[5] P. Grobelny, A. Mukherjee, G.R. Desiraju. *CrystEngComm.*, **13**, 4358 (2011).
[6] R. Kotani, A. Kondo, K. Maeda. *Chem. Commun.*, **48**, 11316 (2012).
[7] E.V. Peresypkina, K.E. Vostrikova. *Dalton Trans.*, 4100 (2012).
[8] J. Cao, K.X. Shang, W.T. Deng, J.C. Liu. *Inorg. Chem. Commun.*, **29**, 183 (2013).
[9] L.H. Zhi, W.N. Wu, Y. Wang, G. Sun. *J. Coord. Chem.*, **66**, 227 (2013).
[10] L. Hashemi, A. Morsali, P. Retailleau. *Inorg. Chim. Acta*, **367**, 207 (2011).
[11] L. Hashemi, A. Morsali. *Inorg. Chim. Acta*, **386**, 56 (2012).
[12] J.M. Burke, J.G. Jurcic, D.A. Scheinberg. *Cancer Control*, **9**, 106 (2002).
[13] M.R. McDevitt, R.D. Finn, D. Ma, S.M. Larson, D.A. Scheinberg. *J. Nucl. Med.*, **40**, 1722 (1999).
[14] J. Cao, J.C. Liu, W.T. Deng, N.Z. Jin. *CrystEngComm.*, **15**, 6359 (2013).
[15] G.M. Sheldrick. *SHELXTL-97, Program for X-ray Crystal Structure Solution*, University of Göttingen, Göttingen, Germany (1997).
[16] C.C. Winterbourn. *Biochem. J.*, **182**, 625 (1979).
[17] C.C. Winterbourn. *Biochem. J.*, **198**, 125 (1981).
[18] L. Shimoni-Livny, J.P. Glusker, C.W. Bock. *Inorg. Chem.*, **37**, 1853 (1998).
[19] V. Stavila, J.C. Fettinger, K.H. Whitmire. *Organometallics*, **26**, 3321 (2007).
[20] V. Stavila, E.V. Dikarev. *J. Organomet. Chem.*, **694**, 2956 (2009).
[21] R.E. Xing, H.H. Yu, S. Liu, W.W. Zhang, Q.B. Zhang, Z.E. Li, P.C. Li. *Bioorg. Med. Chem.*, **13**, 1387 (2005).
[22] Y. Li, Z.Y. Yang, J.C. Wu. *Eur. J. Med. Chem.*, **45**, 5692 (2010).